Nitrogen-14 NMR Study on Solvent Exchange of the Octahedral Cobalt(II) Ion in Neat 1,3-Propanediamine and *n*-Propylamine at Various Temperatures and Pressures. Tetrahedral−Octahedral Equilibrium of the Solvated Cobalt(II) Ion in *n*-Propylamine As Studied by EXAFS and Electronic Absorption Spectroscopy

Sen-ichi Aizawa, Shigeo Iida, Kayoko Matsuda, and Shigenobu Funahashi*

Laboratory of Analytical Chemistry, Faculty of Science, Nagoya University, Chikusa, Nagoya 464-01, Japan

Received July 7, 1995[⊗]

Solvated cobalt(II) ions in neat 1,3-propanediamine (tn) and *n*-propylamine (pa) have been characterized by electronic absorption spectroscopy and extended X-ray absorption fine structure (EXAFS) spectroscopy. The equilibrium between tetrahedral and octahedral geometry for cobalt(II) ion has been observed in a neat pa solution, but not in neat diamine solutions such as tn and ethylenediamine (en). The thermodynamic parameters and equilibrium constant at 298 K for the geometrical equilibrium in pa were determined to be $\Delta H° = -36.1 \pm 2.3$ kJ mol^{-1}, $\Delta S° = -163 \pm 8$ J mol^{-1} K^{-1}, and $K^{298} = 6.0 \times 10^{-3}$ M^{-2}, where $K = [Co(pa)_6^{2+}]/\{[Co(pa)_4^{2+}][pa]^2\}$. The equilibrium is caused by the large entropy gain in formation of the tetrahedral cobalt(II) species. The solvent exchange of cobalt(II) ion with octahedral geometry in tn and pa solutions has been studied by the ^{14}N NMR line-broadening method. The activation parameters and rate constants at 298 K for the solvent exchange reactions are as follows: $\Delta H^{‡} = 49.3 \pm 0.9$ kJ mol^{-1}, $\Delta S^{‡} = 25 \pm 3$ J mol^{-1} K^{-1}, $\Delta V^{‡} = 6.6 \pm 0.3$ cm^3 mol^{-1} at 302.1 K, and $k^{298} = 2.9 \times 10^5$ s^{-1} for the tn exchange, and $\Delta H^{‡} = 36.2 \pm 1.2$ kJ mol^{-1}, $\Delta S^{‡} = 35 \pm 6$ J mol^{-1} K^{-1}, and $k^{298} = 2.0 \times 10^8$ s^{-1} for the pa exchange. By comparison of the activation parameters with those for the en exchange of cobalt(II) ion, it has been confirmed that the kinetic chelate strain effect is attributed to the large activation enthalpy for the bidentate chelate opening and that the enthalpic effect is smaller in the case of the six-membered tn chelate compared with the five-membered en chelate.

Introduction

The solvent exchange studies on metal ions are quite important to understand the kinetics for formation and dissociation of metal complexes and have been extensively performed.[1] We have previously extended these studies to bidentate solvent exchange on the first-row transition metal(II) ions in neat ethylenediamine (en).[2,3] The kinetic chelate strain effect of the en complexes has been attributed to the large activation enthalpy for the dissociative chelate ring opening.[3] Since the metal−nitrogen (M−N) bond in the case of amine nitrogen donors is essentially σ in character, the strength of the bond is sensitive to the degree of overlap of the σ orbitals, which is determined by the orientation of the orbitals observed in the metal−nitrogen−carbon (M−N−C) angle.[4] It has been claimed that the elongation of the M−N bond in the opening process of the en chelate ring decreases the M−N−C angle and highly weakens the σ bonding.[3] However, in the case of the activation of monodentate amine solvents, there is no such angular distortion around the leaving nitrogen donor.

An investigation of diamine solvents with different chelate ring size may provide further insight into the kinetic chelate strain effect on bidentate solvent exchange. Enlargement of the chelate ring, for example, may release the distortion of the leaving amine nitrogen in the transition state and may decrease the activation energy. Therefore, we selected 1,3-propanediamine (trimethylenediamine, tn) as a bidentate solvent that forms a six-membered chelate ring, in order to make a comparison with the results for the en exchange. To clarify the difference between bidentate and monodentate solvents, we also studied the exchange reaction of *n*-propylamine (pa) as a monodentate solvent. This appears to be the first instance for the solvent exchange of a monodentate alkylamine. Cobalt(II) ion was chosen among the first-row transition metal(II) ions that were previously studied for the en exchange[3] because electronic spectra of its complexes can conveniently provide structural informations. This has been useful in the present work to study the tetrahedral−octahedral equilibrium that has been observed in the cobalt(II)−pa system.

Experimental Section

Solvents. 1,3-Propanediamine (tn, Wako, Pr. Gr.) was kept for a few days in the presence of activated 4A molecular sieves. The supernatant liquid was decanted and then agitated for a day in the presence of calcium oxide and potassium hydroxide, which was then distilled under vacuum over activated 4A molecular sieves. The resultant tn was dried over sodium and distilled under vacuum. *n*-Propylamine (pa, Wako, Special Gr.) was kept for a few days in the presence of activated 4A molecular sieves and zinc powder and then distilled twice at atmospheric pressure. The resultant pa was dried over sodium and then distilled under vacuum. The solvents were distilled just before use.

Anhydrous Cobalt(II) Trifluoromethanesulfonate. Basic cobalt(II) carbonate (Wako, Pr. Gr.) was dissolved in an aqueous solution

[⊗] Abstract published in *Advance ACS Abstracts*, February 1, 1996.

(1) (a) Wilkins, R. G. *Kinetics and Mechanism of Reactions of Transition Metal Complexes*; VCH: Weinheim, Germany, 1991. (b) Burgess, J. *Metal Ions in Solution*; Ellis Horwood: New York, 1978.
(2) Soyama, S.; Ishii, M.; Funahashi, S.; Tanaka, M. *Inorg. Chem.* **1992**, *31*, 536.
(3) Aizawa, S.; Matsuda, K.; Tajima, T.; Maeda, M.; Sugata, T.; Funahashi, S. *Inorg. Chem.* **1995**, *34*, 2042.
(4) Douglas, B.; Hollingsworth, C. A. *Symmetry in Bonding and Spectra*; Academic Press: San Diego, CA, 1985; Chapter 8. According to the angular overlap model, the π-interaction energy also shows the angular dependence. However, the π interaction of the amine nitrogen donor is negligible. If the donor atom has a π interaction, the discussion of the change in bond strength is not straightforward.

0020-1669/96/1335-1338$12.00/0

of trifluoromethanesulfonic acid (triflic acid, Wako, 98%). The residue was removed by filtration, and the filtrate was concentrated to obtain the crystals of hexaaquacobalt(II) trifluoromethanesulfonate (triflate). The aquacobalt(II) triflate was dried at 300 °C for 3 h to obtain the anhydrous salt. The dehydration conditions were decided by thermogravimetry with a VT-30 Shimadzu thermal analyzer, and the formation of the anhydrous salt was confirmed by the EDTA titration using Xylenol Orange as an indicator.[5]

Sample Preparation. Sample preparations for NMR measurements were carried out under dry nitrogen in a glovebox and on a vacuum line. Sample solutions for tn exchange measurements were prepared in a glovebox by dissolving known amounts of anhydrous cobalt(II) triflate in freshly distilled tn. The tn solutions for variable-temperature NMR measurements were transferred into 5 mm o.d. NMR tubes in a glovebox that were then flame-sealed after degassing on a vacuum line. The tn solution for variable-pressure NMR measurements was transferred into a 7 mm o.d. NMR tube that was then capped with a flexible Teflon tube in a glovebox as previously described.[6,7] Because of the higher oxygen sensitivity of the pa solution compared with the tn solution, the variable-temperature NMR samples for pa exchange measurements were prepared by vacuum distillation of purified pa into 5 mm o.d. NMR tubes containing anhydrous cobalt(II) triflate that were then flame-sealed after degassing. The concentrations of cobalt(II) ion in the pa sample solutions were determined by EDTA titration after completion of the NMR measurements. Unfortunately, the variable-pressure NMR sample for pa exchange measurements might be oxidized during a preparation procedure similar to that for the tn exchange. The compositions of sample solutions are given in Table S1 (Supporting Information).

The tn sample solution for absorption spectral measurements was prepared in a glovebox using a quartz cuvette with a path length of 1 cm with a Teflon cap. The pa sample solutions were prepared on a vacuum line by a procedure similar to that for the NMR samples of the pa solutions using quartz cuvettes, which were then flame-sealed. The concentrations of cobalt(II) ion in the pa solutions were determined by EDTA titration after the measurements.

Sample solutions of ca. 0.3 mol dm^{-3} for EXAFS measurements were prepared by dissolving known amounts of anhydrous cobalt(II) triflate in freshly distilled tn and pa in a glovebox, and the sample glass tubes containing the sample solutions were flame-sealed after degassing on a vacuum line. Just before EXAFS measurements, a glass filter disk was immersed in each sample solution and doubly sealed in PET (poly(ethyleneterephthalate), Toray Co.) film bags in a glovebox.

Measurements. The ^{14}N NMR measurements at various temperatures and pressures were performed on a JEOL JNM-GX270 FT-NMR spectrometer operating at 19.52 MHz. The sample tubes for various temperature NMR measurements were coaxially mounted in 10 mm o.d. NMR tubes containing deuterated acetone, water, or dimethyl sulfoxide as a lock solvent. The temperature was measured by a substitution technique using a thermistor (D641, Takara Thermistor Co.) or a copper−constantan thermocouple. About 15 min was required for the temperature equilibration of the sample solution and the temperature stability was ±0.1 K. The various pressure NMR measurements were carried out by using a high-pressure NMR probe constructed for the wide-bore superconducting magnet (6.34 T) of a JEOL JNM-GX270 FT-NMR spectrometer as previously described.[3,6,7]

Electronic absorption spectra were recorded on Shimadzu UV-3100PC and UV-265FW spectrophotometers. For the equilibrium experiments, the temperature of solutions was controlled within ±0.1 K. The unit of M^{-1} cm^{-1} (M ≡ mol dm^{-3}) is used for a molar absorption coefficient (ϵ) where the unit of mol kg^{-1} was converted to mol dm^{-3} with knowledge of the density of the solutions. The densities of pa solvent at various temperatures were measured with an Anton Paar DMA 60 digital density meter.

EXAFS spectra were measured around the cobalt K edge using the BL6B station at the Photon Factory of the National Laboratory for High Energy Physics.[8] The monochromatized X-ray was obtained by an Si(111) double crystal. The incident X-ray intensity I_0 and the transmitted X-ray intensity I were simultaneously measured with the ionization chamber filled with nitrogen gas and nitrogen/aron (85:15) mixture, respectively.

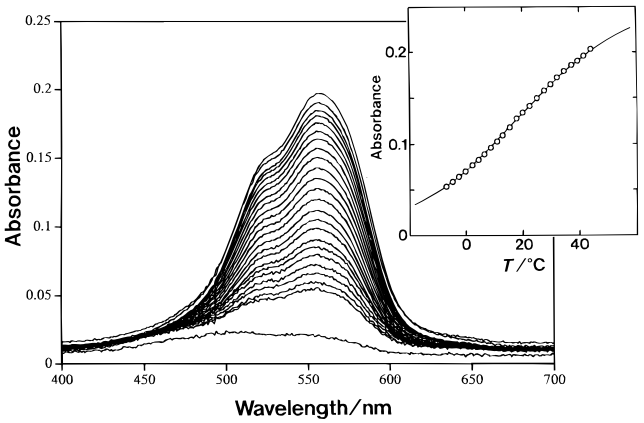

Figure 1. Visible absorption spectra for pa solution of cobalt(II) ion at various temperatures: 317.0, 314.4, 312.5, 310.4, 307.9, 305.4, 303.0, 300.5, 298.1, 295.6, 293.2, 290.8, 288.6, 286.0, 284.2, 281.9, 279.6, 277.3, 275.1, 272.9, 270.5, 268.1, 266.4, and below 243 K from upper spectra. $C_{Co} = 1.35 \times 10^{-3}$ mol dm^{-3}. The inset shows the temperature dependence of absorbance at 555 nm. The solid line is depicted using the obtained values of the thermodynamic parameters and molar absorption coefficients.

Results

Equilibrium Study. Figure 1 shows a series of visible absorption spectra for a pa solution of cobalt(II) ion at various temperatures. On the assumption that the reversible change in the visible absorption spectra with temperature variation is attributed to the tetrahedral−octahedral (tet/oct) equilibrium for cobalt(II) ion as expressed by eq 1 (*vide infra*), absorbance (A) at a given wavelength as a function of temperature is given by eqs 2 and 3, where $[Co]_t$ is the total concentration of Co(II)

$$[Co(pa)_4]^{2+}(tet) + 2pa \rightleftarrows [Co(pa)_6]^{2+}(oct) \qquad (1)$$

$$A = K'[Co]_t(\epsilon_{oct}-\epsilon_{tet})/(1+K') + \epsilon_{tet}[Co]_t \qquad (2)$$

$$K' = \exp(-\Delta H°/RT + \Delta S°'/R) \qquad (3)$$

ion, K' is the ratio of the concentration of the octahedral species to that of the tetrahedral species, and ϵ_{oct} and ϵ_{tet} are the respective molar absorption coefficients. The cobalt(II) concentration at each temperature was corrected to the molar scale by using the density of pa solvent at the corresponding temperature as described in the Experimental Section.[9] The equilibrium data were analyzed by means of eqs 2 and 3 using 23 points over the temperature range 266−317 K at 555 nm to give a good fit to the calculated curve (the inset in Figure 1 and Table S2). The thermodynamic parameters and equilibrium constant at 298 K were determined to be $\Delta H° = -36.1 \pm 2.3$ kJ mol^{-1}, $\Delta S°' = -122 \pm 8$ J mol^{-1} K^{-1}, and $K'^{298} = 0.87$. For the equilibrium constant $K = [Co(pa)_6^{2+}]/\{[Co(pa)_4^{2+}][pa]^2\}$ where [pa] = 12.05 M at 298 K, the values of $\Delta S°$ and K^{298} are evaluated to be -163 ± 8 J mol^{-1} K^{-1} and $K^{298} = 6.0 \times 10^{-3}$ M^{-2}, respectively. These values obtained at 555 nm are in good agreement with those obtained at 525, 545, and 565 nm. Such an equilibrium was not observed for the cobalt(II) ion in tn.

(5) Koros, E.; Remport-Horrath, Z. *Chem.-Anal.* **1957**, *46*, 91.
(6) Ishii, M.; Funahashi, S.; Ishihara, K.; Tanaka, M. *Bull. Chem. Soc. Jpn.* **1989**, *62*, 1852.
(7) Funahashi, S. *High Pressure Liquids and Solutions*; Taniguchi, Y., Senoo, M., Hara, K., Eds.; Elsevier: Amsterdam, 1994; pp 31−48.
(8) Nomura, M. *KEK Report 85−7*; National Laboratory for High Energy Physics: Tsukuba, Japan, 1985.
(9) The densities of pa at 3.7, 13.7, 24.1, 34.3, and 43.8 °C are 0.732, 0.724, 0.713, 0.701, and 0.690 g cm^{-3}, respectively.

EXAFS Study. The outline of the EXAFS analysis is as follows.[10,11] The background absorption was estimated by fitting the Victoreen formula to the data in the pre-edge region,[12] and the smooth K shell absorption (μ_0) was approximated by the sixth-order polynomial function. The values of extracted absorbance were normalized by μ_0 and were converted to the EXAFS oscillation, $\chi(k)$. The photoelectron wave vector k is equal to $\{8m(E - E_0)\}^{1/2}\pi/h$, where E is the energy of the incident X-ray, E_0 is the threshold energy of a K-shell electron, m is the mass of the electron, and h is the Plank constant. The model function of EXAFS oscillation was fitted to the Fourier filtered $k^3\chi(k)$ values by a least-squares calculation over the range $4 < k/10^{-2}\ \mathrm{pm}^{-1} < 11$. The reported values were used for the backscattering amplitude and total scattering phase shift.[13] The observed EXAFS oscillations $\chi_{obsd}(k)$ weighted by k^3, the Fourier transforms $|G(R)|$ of $k^3\chi_{obsd}(k)$, and the Fourier filtered EXAFS oscillations $\chi(k)$ for water, tn, and pa solutions of the cobalt(II) ion are given in Figure 2A−C, respectively.

Values of E_0 and the mean free path of a photoelectron, λ, were evaluated by use of the EXAFS data for the aqueous solution of $[Co(H_2O)_6](CF_3SO_3)_2$ as a standard sample by fixing the scatterer number n to 6, because the six-coordinate octahedral structure of aquacobalt(II) ion has been confirmed.[14] The obtained values, 7.7234 keV for E_0 and 528 pm for λ, were kept constant for the structural analyses for the tn and pa solutions. The interatomic distance R, the Debye−Waller factor σ, and n as variables were optimized for the tn solution. On the assumption that both octahedral and tetrahedral cobalt(II) species exist in the pa solution at ambient temperature (vide supra), the structural analysis was performed by considering two different Co-N distances. The structure parameters obtained are listed in Table 1 together with those for $[Co(H_2O)_6]^{2+}$.

NMR Study. The NMR line-broadening of solvent molecules in the bulk due to the paramagnetic ion is expressed as $T_{2P}^{-1} = \pi(\Delta\nu_{obsd} - \Delta\nu_{solv})$, where T_{2P}^{-1} is the transverse relaxation rate and $\Delta\nu_{obsd}$ and $\Delta\nu_{solv}$ are the half-height widths of the NMR spectra of the solvent molecules in the bulk in the presence and absence, respectively, of the paramagnetic ion. Because the transverse relaxation rate was confirmed to be proportional to the cobalt(II) ion concentration, the T_{2P}^{-1} value was normalized by dividing by the molar fraction of bound solvent molecules, P_M. The NMR line broadening data were analyzed by means of the modified Swift−Connick equation[15,16]

$$\frac{1}{T_{2P}P_M} = \left(\frac{1}{\tau_M}\right)\frac{T_{2M}^{-2} + (\tau_M T_{2M})^{-1} + (\Delta\omega_M)^2}{(\tau_M^{-1} + T_{2M}^{-1})^2 + (\Delta\omega_M)^2} + \frac{1}{T_{2o}} \quad (4)$$

in which the symbols have their usual meanings.[17] In the case of the pa solutions of cobalt(II) ion, the NMR data at temperatures below 244 K were used for the analysis, where the octahedral cobalt(II) species exists predominantly (>96%) on the basis of the results of the equilibrium experiments (*vide supra*). Figure 3 shows the temperature dependences of $(T_{2P}P_M)^{-1}$ for the ^{14}N nucleus of tn and pa, and all the line-broadening data are deposited, respectively, in Tables S3 and S4 (Supporting Information). As apparent from Figure 3, the τ_M^{-1} and $\tau_M(\Delta\omega_M)^2$ terms dominate the relaxation over the present temperature range, and T_{2M}^{-1} and T_{2o}^{-1} are small compared to the other relaxation terms. Thus, eq 4 is reduced to

$$(T_{2P}P_M)^{-1} = (\tau_M^{-1}(\Delta\omega_M)^{-2} + \tau_M)^{-1} \quad (5)$$

The solvent exchange rate constant k_{ex} is equal to $\tau_M^{-1} = (k_B T/h)\exp(-\Delta H^{\ddagger}/RT + \Delta S^{\ddagger}/R)$. The temperature dependence of

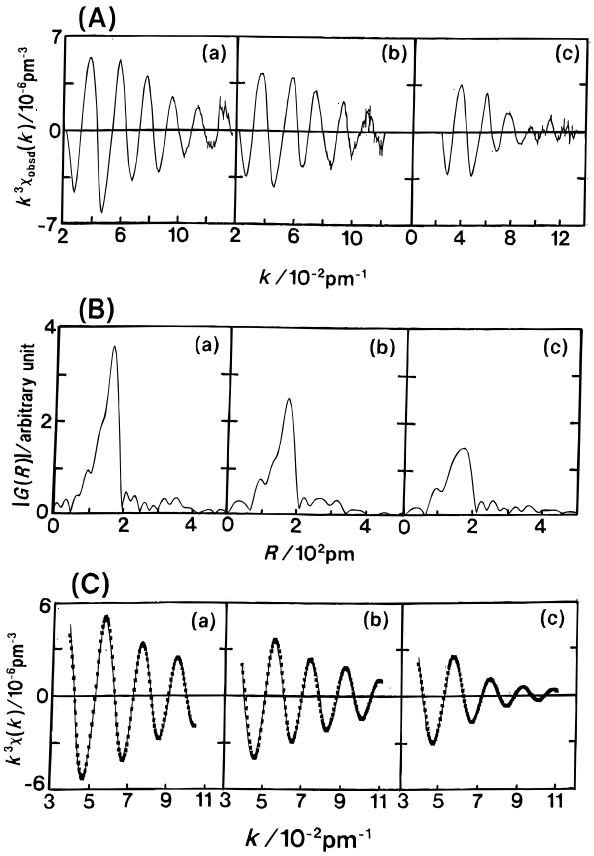

Figure 2. EXAFS spectra for aqueous (a), tn (b), and pa (c) solutions of cobalt(II) ion: (A) observed EXAFS oscillation $\chi_{obsd}(k)$ weighted by k^3; (B) Fourier transforms $|G(R)|$ of $k^3\chi_{obsd}(k)$, uncorrected for the phase shift; (C) Fourier filtered EXAFS oscillations. For part B, the $k^3\chi_{obsd}(k)$ values depicted in Figure 2A were converted to the radial distribution function $G(R)$ by the Fourier transformation: $G(R) = (1/2\pi)^{1/2}\int_{k_{min}}^{k_{max}} k^3[\chi_{obsd}(k)][W(k)]\exp(-2ikR)\,dk$, where $W(k)$ is a window function. For part C, the squares are $k^3\chi(k)$ values obtained by the inverse Fourier transformation for $|G(R)|$ in Figure 2B, and the solid lines are $k^3\chi_{calcd}(k)$ curves calculated by using the parameters in Table 1 according to the following equation: $\chi_{calcd}(k) = \sum(n_j/kR_j^2)\exp(-2\sigma_j^2k^2 - 2R_j/\lambda)\,F_j(\pi,k)\sin(2kR_j - \alpha_j(k))$, where $F_j(\pi,k)$ is the backscattering amplitude from each of scatterer j at a distance R_j from the X-ray absorbing atom and $\alpha_j(k)$ is the total scattering phase shift experienced by the photoelectron.[12]

Table 1. Structure Parameters for Solvated Cobalt(II) Ions in Water, tn, and pa[a]

solvent	R/pm[b]	σ/pm[c]	n[d]
water	208(1)	6.9(0.2)	6[e]
tn	217(1)	7.3(0.2)	6.1(0.2)
pa	217(1)	7.3[e]	4.3(0.2)
	201(1)	5.0(0.2)	1.3(0.2)

[a] The standard deviations are given in parentheses. [b] The interatomic distance between cobalt(II) ion and coordinated atoms. [c] The Debye−Waller factor. [d] The number of scatterers. [e] Fixed value.

(10) (a) Ozutsumi, K.; Kawashima, T. *Inorg. Chim. Acta*, **1991**, *180*, 231. (b) Ozutsumi, K.; Miyata, Y.; Kawashima, T. *J. Inorg. Biochem.* **1991**, *44*, 97.
(11) Inada, Y.; Sugimoto, K.; Ozutsumi, K.; Funahashi, S. *Inorg. Chem.* **1994**, *33*, 1875.
(12) *International Tables for X-ray Crystallography*; Kynoch Press: Birmingham, U.K., 1962; Vol. III, p 161.
(13) Teo, B. K.; Lee, P. A. *J. Am. Chem. Soc.* **1979**, *101*, 2815.
(14) (a) Marcus, Y. *Chem. Rev.* **1988**, *88*, 1475. (b) Ohtaki, H.; Radnai, T. *Chem. Rev.* **1993**, *93*, 1157.
(15) Swift, T.; Connick, R. E. *J. Chem. Phys.* **1962**, *37*, 307.
(16) Rusnak, L. L.; Jordan, R. B. *Inorg. Chem.* **1976**, *15*, 709.
(17) Hioki, A.; Funahashi, S.; Tanaka, M. *J. Phys. Chem.* **1985**, *89*, 5057.

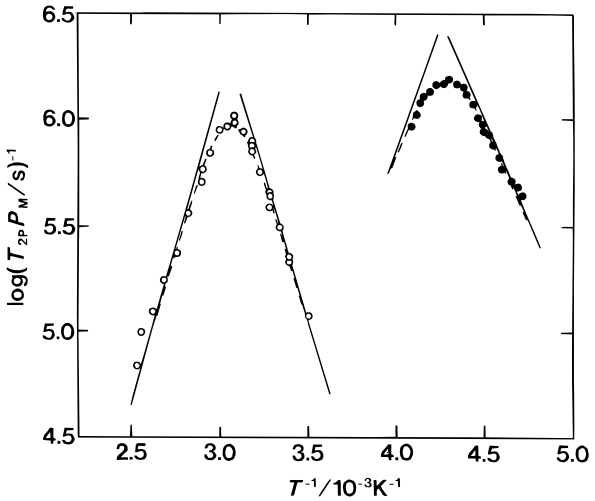

Figure 3. Temperature dependence of $\log(T_{2P}P_M)^{-1}$ for 19.52-MHz ^{14}N NMR in tn (○) and pa (●) solutions. $P_M = 1.23 \times 10^{-2}$ and 4.92×10^{-3} for the tn solution and $P_M = 2.47 \times 10^{-3}$ and 8.62×10^{-4} for the pa solution. The solid lines with negative and positive slopes indicate the contributions of τ_M^{-1} and $\tau_M\Delta\omega_M^2$ terms, respectively.

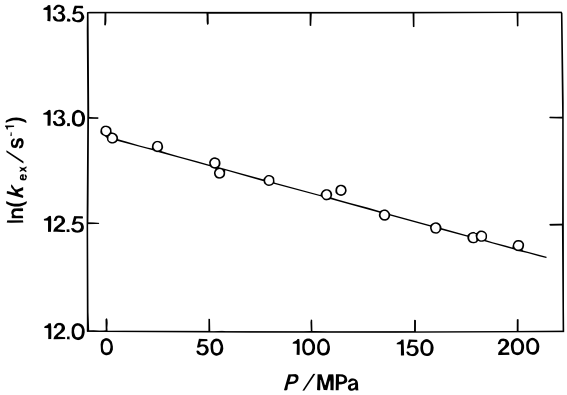

Figure 4. Pressure dependence of k_{ex} for tn exchange of cobalt(II) ion at 302.1 K.

$\Delta\omega_M$ is expressed as $\Delta\omega = -C_\omega/T$. All the parameters obtained by least-squares fitting according to eq 5 are listed in Table S5.

The variable-pressure ^{14}N NMR experiments for the tn solution of cobalt(II) ion have been performed at 302.1 K where $(T_{2P}P_M)^{-1}$ is equal to k_{ex}. From the transition-state theory, the activation volume, $\Delta V^{\ddagger}$, is given by the relation, $(\partial(\ln k_{ex})/\partial P)_T = -\Delta V^{\ddagger}/RT$. Since the plot of ln k_{ex} vs P is linear within experimental errors (Figure 4 and Table S6), the $\Delta V^{\ddagger}$ value was determined from the slope to be 6.6 ± 0.3 cm^3 mol^{-1}. The activation parameters and rate constants at 298 K for the tn and pa exchange on the cobalt(II) ion are summarized in Table 2 together with those for the en exchange.

Discussion

The electronic absorption spectrum for the neat tn solution of cobalt(II) ion is quite similar to that for $[Co(en)_3]^{2+}$,[3,18] exhibiting three absorption bands with weak intensity ($\epsilon = 3-12$ M^{-1} cm^{-1}) assigned to the transitions from $^4T_{1g}$ to $^4T_{2g}$, $^4A_{2g}$, and $^4T_{2g}$(P) for the high-spin d^7 ion with octahedral geometry. The neat pa solution of cobalt(II) ion shows the corresponding three absorption bands at temperatures below 238 K, while the spectrum for the solution at higher temperature becomes characteristic of the tetrahedral cobalt(II) species with strong intensity.[19] The absorption spectral data are summarized in Table 3. Following the standard analysis,[19] the crystal field strength, 10*Dq*, and the Racah parameter, *B*, for the high-spin d^7 ion in an octahedral field can be estimated from the electronic transition energies (Table 3). The order of increase in the *B* values, en < tn < pa, may correspond to the electron density of the amine nitrogen donors. However, it is notable that the order of 10*Dq*, en < tn < pa, is different from the order of the crystal field strength for the cobalt(III) complexes, tn < NH_3 < en, established from the d−d transition energy of $^1A_{1g} \rightarrow {}^1T_{1g}$ and $^1A_{1g} \rightarrow {}^1T_{2g}$.[19,20] The ion radius of cobalt(III) is suitable for the chelate ring size of en with the energetically favorable gauche conformation, while the six-membered tn chelate is obviously large for cobalt(III) ions.[3,21] The fitness of ion radius to the chelate ring size is reflected in the distortion of the M−N−C angles, which sensitively affects the overlap of the σ bonding orbitals,[3,4] and consequently, the crystal field strength. On the other hand, we have pointed out that the ion radius of cobalt(II) ion is significantly large for the en chelate ring.[3] This finding is consistent with the relatively weak crystal field for the en ligand compared to the tn and pa ligands.

Table 2. Kinetic Parameters for Solvent Exchange of Cobalt(II) Ion in en, tn, and pa

solvent	k_{ex}^{298}/s^{-1}	$\Delta H^{\ddagger}$/kJ mol^{-1}	$\Delta S^{\ddagger}$/J mol^{-1} K^{-1}	$\Delta V^{\ddagger}$/cm^3 mol^{-1}
en[a]	5.4×10^3	56.5 ± 3.3	16 ± 10	0.9 ± 0.9[b]
tn[c]	2.9×10^5	49.3 ± 0.9	25 ± 3	6.6 ± 0.3[d]
pa[c]	2.0×10^8	36.2 ± 1.2	35 ± 6	
H_2O[e]	3.2×10^6	46.9	37.2	6.1
CH_3OH[e]	1.8×10^4	57.5	30.1	8.9
CH_3CN[e]	3.4×10^5	49.5	27.1	9.9
NH_3[e]	5.0×10^7	45.8	31.2	

[a] Reference 3. [b] At 332.4 K. [c] This work. [d] At 302.1 K. [e] Reference 25.

It is possible for anionic ligands with the weak crystal field to form tetrahedral cobalt(II) complexes such as tetrahalogeno complexes, even if there is no steric repulsion.[19] Interestingly, $[Co(pa)_4]^{2+}$ is the first instance of the tetrahedral cobalt(II) complex with strong aliphatic amine donors in a solution though the tetraammine cobalt(II) complex in the solid state is available.[22]

The finding that such a tet/oct equilibrium for the bidentate primary amines of en and tn was not observed is referred to the contribution of the steric and/or entropical factors as follows. Formation of a bis(diamine)cobalt(II) complex with the distorted tetrahedral geometry of small chelate bite angles should be unfavorable. On the other hand, rearrangement from an octahedral tris(diamine) complex to a tetrahedral tetrakis(diamine) complex by binding of an additional diamine ($[Co(diamine)_3]^{2+}$ + diamine → $[Co(diamine)_4]^{2+}$) should be entropically unfavorable compared with the reaction of a monodentate amine complex ($[Co(amine)_6]^{2+} \rightarrow [Co(amine)_4]^{2+}$ + 2 amine). Thus, the appearance of the tetrahedral complex for the pa system is caused by the large entropy gained in releasing two pa molecules.

The *n* of 6.1 ± 0.2 obtained by the EXAFS method for the tn solution is consistent with the octahedral geometry supported by the absorption spectrum, and the *R* of 217 ± 1 pm is in reasonable agreement with the Co−N bond distance for $[Co(en)_3]^{2+}$, 218 pm, previously estimated.[3] For the pa solution,

(18) Yang, M. C.-L.; Palmer, R. A. *J. Am. Chem. Soc.* **1975**, *97*, 5390.
(19) Lever, A. B. P. *Inorganic Electronic Spectroscopy*, 2nd ed.; Elsevier: Amsterdam, 1984; Chapters 3 and 6.
(20) Ogino, H.; Fujita, J. *Bull. Chem. Soc. Jpn.* **1975**, *48*, 1836.
(21) Nagao, R.; Marumo, F.; Saito, Y. *Acta Crystallogr.* **1973**, *B29*, 2438.
(22) Muller, A.; Christophliemk, P.; Tossidis, I. *J. Mol. Struct.* **1973**, *15*, 289.

Table 3. Absorption Spectral Data for Solvated Cobalt(II) Ions in en, tn, and pa[a]

	$[Co(en)_3]^{2+}$ [b]	$[Co(tn)_3]^{2+}$ [c]	$[Co(pa)_6]^{2+}$ [c]	$[Co(pa)_4]^{2+}$ [c–e]
$^4T_{1g} \rightarrow {}^4T_{2g}$	9.97 (4.3)	9.70 (3.5)	8.55 (7)	
$^4T_{1g} \rightarrow {}^4A_{2g}$	18.73 (4.5 sh)	18.52 (4.9 sh)	17.76 (10 sh)	
$^4T_{1g} \rightarrow {}^4T_{2g}(P)$	20.62 (12.1)	20.45 (12.1)	19.49 (15)	
$^4A_2 \rightarrow {}^4T_1(F)$				8.40 (46)
$^4A_2 \rightarrow {}^4T_1(P)$				17.67 (213), 18.66 (163 sh)
$10Dq/10^3$ cm^{-1}	8.76	8.82	9.21	
$B/10^3$ cm^{-1}	0.63	0.66	0.77	

[a] Wave numbers and ϵ (in parentheses) are given in 10^3 cm^{-1} and M^{-1} cm^{-1}, respectively. [b] Reference 3. [c] This work. [d] The values of ϵ were evaluated from the equilibrium data. [e] The absorption band assigned to the transition from $^4A_2$ to $^4T_2$ was not observed because of overlapping with the strong absorption of the solvent.

Scheme 1

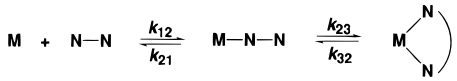

two distinct R values were obtained. The larger R of 217 ± 1 pm is equal to that for the tn solution and the smaller R of 201 ± 1 pm is smaller by 16 pm that corresponds to the difference of 16.5 pm in the effective ion radii of cobalt(II) ion between high-spin octahedral and tetrahedral geometry.[23] Furthermore, the percentages of the two species with the coordination number of 6 and 4 in the pa solution are 72 ± 3 and 33 ± 5%, respectively, and their sum is reasonably equal to ca. 100%.[24] These EXAFS results are compatible with those in tn and pa solutions indicated by the absorption spectra and the equilibrium experiments. The subtle difference in the crystal field strength among the en, tn, and pa cobalt(II) complexes is not observed in the Co−N bond distances.

As above described, there is not large difference in the Co−N bond distance and crystal field strength in the ground state for the six-coordinate Co(II) ion in pa, tn, and en. Furthermore, as apparent from the values of $\Delta S^{\ddagger}$ and $\Delta V^{\ddagger}$ in Table 2, these primary amine donor solvents are dissociatively activated in common with the other solvents.[25] However, the wide variation of rate constants at 298 K for the pa, tn, and en exchanges comes from the large difference in $\Delta H^{\ddagger}$, ranging from 36.2 to 56.5 kJ mol^{-1}. Thus, we can expect enthalpically different activation process among the three amine systems. We have claimed that, in the dissociative transition state of the en exchange, elongation of the M−N bond should decrease the M−N−C bond angle and highly weaken the σ bonding, compared to monodentate amine ligands having no angular distortion around the leaving nitrogen donor. Such a difference in the activation state is verified by the large difference in $\Delta H^{\ddagger}$ for the en and pa exchange as an origin of the kinetic chelate strain effect. Another important point is that the kinetic chelate strain effect is sensitive to the chelate ring size as shown by the distinct values of $\Delta H^{\ddagger}$ for the en and tn exchange. The five-membered en chelate is forced to have a quite distorted M−N−C angle in the dissociatively activated process, while the six-membered tn chelate can flexibly elongate the M−N bond to form a less distorted M−N−C angle in which the σ orbitals between the metal ion and nitrogen donor is overlapped more largely. Though difference in the values of $\Delta S^{\ddagger}$ in the present system is, in fact, observed,[3] such an entropic effect is a minor factor for the large difference in the activation energy.

In addition, we can review the thermodynamic chelate effect for the different size of chelate rings on the basis of the present discussion about the kinetic chelate strain effect. Scheme 1 shows the chelate formation process for the diamine complexes and the formation constant is given by eq 6. The values of K_f

$$K_f = k_{12}k_{23}/k_{21}k_{32} \qquad (6)$$

for the transition metal(II) complexes of tn are smaller than those for the corresponding complexes of en in spite of the higher basicity of tn.[26] Such discrepancy between the five-membered and six-membered chelate rings in partially attributed to the difference in rate for the chelate ring closing (k_{23}) of bidentate en and tn due to the entropic effect. However, in the previous paper,[3] we have pointed out that the smaller rate constants of chelate ring opening (k_{32}) due to the enthalpic effect significantly contribute to the larger formation constants of the chelate complexes. It should be noted here that the difference in the enthalpic kinetic effect between the en and tn complexes is significant when interpreting the lower stability of the tn complexes compared with the en complexes. These findings can be applied to the chelate complexes in which the σ bonding mainly operates.[4]

Acknowledgment. The EXAFS measurements were performed under the approval of the Photon Faculty Program Advisory Committee (Proposal No. 92G179). This research was supported by Grants-in-Aid for Scientific Research (Nos. 06640779, 07454199, and 07504003) from the Ministry of Education, Science, and Culture of Japan. S. A. gratefully acknowledges receipt of a grant from the Kurata Foundation.

Supporting Information Available: Composition of the NMR sample solutions (Table S1), equilibrium data for pa solution (Table S2), NMR line-broadening data at various temperatures for tn exchange (Table S3) and pa exchange (Table S4), values of $\Delta H^{\ddagger}$, $\Delta S^{\ddagger}$, and C_{ω} (Table S5), and NMR line-broadening data at various pressures for tn exchange (Table S6) (4 pages). Ordering information is given on any current masthead page.

IC950855Q

(23) Shannon, R. D. *Acta Crystallogr*. **1976**, *A32*, 751.
(24) The *n* value in Table 1 corresponds to the product of the coordination number and the mole ratio of each species.
(25) Jordan, R. B. *Reaction Mechanisms of Inorganic and Organometallic Systems*; Oxford University Press: New York, 1991; Chapter 3. The original references are cited therein.
(26) Smith, R. M.; Martell, A. E. *Critical Stability Constants*, Plenum Press: New York, 1975; Vol. 2.